1

Improved cyclohexanone vapor detection via gravimetric sensing

Aida R. Colón-Berríos, Christine K. McGinn, *Student Member, IEEE*, Marco R Cavallari, *Member, IEEE*, José A. Bahamonde, Natallia Yelavik, Hannes Mikula, Johannes Bintinger, and Ioannis Kymissis, *Senior Member, IEEE*,

Abstract—Functionalized gravimetric sensors are a promising path to small, versatile, real-time vapor sensors for volatile organic compounds. Many of these compounds can be dangerous to human health, but their nonreactive nature makes them notoriously difficult to sense. Unlike bulk acoustic resonators, chemiresistive devices have been investigated extensively and many researchers have used innovative synthesis strategies to functionalize these devices. In this work, we demonstrate how modifying a particular sensitizer for use with a bulk acoustic resonator significantly improves the sensitivity of the device (5 ppm vs. 1.11 ppm). Additionally, readout circuitry is described to avoid some problems that typically plague gravimetric sensors while simplifying the overall system. These strategies create a playbook for simple, fast, and sensitive systems for sensing volatile organic compounds, while also demonstrating the lowest limit of detection for cyclohexanone outside of gas chromatography/mass spectrometery in the literature.

Index Terms—bulk acoustic wave resonator, gravimetric sensor, MEMS sensor, explosive detection, cyclohexanone

I. Introduction

Volatile organic compounds (VOCs) are chemicals with moderate molecular mass and high vapor pressure that are found in gas form at room temperature [1]. These compounds can be found in organic solvents, exhaust gases, decaying plants, and flesh. [2]–[4] VOC sensing can be used for many applications ranging from threat detection to sensing indoor air quality, monitoring food freshness, and evaluating health through breath. [5]–[7]

Threat detection (e.g. of explosives and chemical weapons) through sensing VOCs is an area of particular interest, and can be achieved by sensing the VOCs associated with fabricating explosives and their precursors. Cyclotrimethylene trinitramine (RDX) is a commonly used shock sensitive plastic explosive. With a higher explosive energy than TNT, moderate toxicity, and possible carcinogenicity to humans, detecting this material is of great interest for human safety. [8] Unfortunately, RDX has a low vapor pressure of approximately 5 ppt at room temperature, which makes detection in the gas phase challenging.

Corresponding author: Christine McGinn, email: cm3592@columbia.edu A.R. Colón-Berrios, J.A. Bahamonde, C.K. McGinn, M.R. Cavallari, and I. Kymissis are with the Department of Electrical Engineering, Columbia University, New York, USA.

M.R. Cavallari is with Departamento de Engenharia de Sistemas Eletr ônicos, Escola Politécnica da Universidade de São Paulo, São Paulo, Brazil and Department of Renewable Energies. UNILA, Federal University of Latin American Integration, Av. Sílvio Américo Sasdelli, 1842 Foz do Iguaçu, PR, Parail

N. Yellavik, H. Mikula, and J. Bintinger are with Institute of Applied Synthetic Chemistry, TU Wien, Vienna, Austria. J. Bintinger is also with Austrian Institute of Technology, Tulln, Austria.

Cyclohexanone, a solvent used in the recrystallization process used to make RDX shock sensitive, has a high vapor pressure and evolves from plastic explosives with an atmospheric concentration on the order of 5000 ppm. Its detection is considered a sign of the presence of RDX. [8], [9]

Previous work in threat detection via VOC sensing has largely made use of mass spectrometry and gas chromatography to identify dangerous VOCs accurately and rapidly. [10], [11] Mass spectrometry, however, requires expensive, bulky equipment and is difficult to use in real time [12]. Efforts have been made to fabricate portable sensing units and to also take advantage of MEMS technology to decrease device size [13], [14]. Significant progress has also been made with electrochemical sensors, specifically chemiresistors and field effect transistors, to detect these components [15]–[17]. These devices have demonstrated parts per million limits of detection and the ability to differentiate between several different VOCs. [18] Many of these technologies take advantage of low dimensional materials for their high surface area to volume ratio, but these materials can be expensive and difficult to use in device fabrication. [19], [20] Additionally, substantial calibration is often needed to differentiate between different analytes. [18] Several optical gas sensors are commercially available, but these are sensitive to contamination of the optics. [12]

A promising approach to vapor sensing is mass loading based on MEMS technology, and several reviews have covered these efforts. [21], [22] Several types of MEMS, including surface acoustic wave resonators, bulk acoustic wave resonators, microcantilevers, and quartz crystal monitors, have been used in gas sensors with parts per million limits of detection or lower. [23]–[25] Bulk acoustic resonators, in particular solidly mounted resonators, offer many of the same advantages of other devices like surface acoustic wave resonators including the presence of no moving parts and low power consumption, but they have been less widely studied for vapor sensing applications. [12] The GHz-range resonant frequency and low loss of bulk acoustic resonators allows for high sensitivity with low power consumption. In addition, the small format package enables integration with space and power-constrained portable devices. [26]

A large number of artificial receptors have been developed for use in chemiresistive and optical sensing modalities. [27]. Many of these receptors can be directly used in a gravimetric mode, relaxing the need for optical or electrical functionality and allowing for higher sensitivity, straightforward integration with portable devices, and array co-integration. In particular, use of a self-assembled monolayer (SAM) provides a faster

Fig. 1. (a) Absorption mechanism of thiourea group (left) for cyclohexanone. Reprinted with permission from K. M. Frazier and T. M. Swager, "Robust cyclohexanone selective chemiresistors based on single-walled carbon nanotubes," Anal. Chem., vol. 85, no. 15, pp. 7154–7158, 2013. Copyright 2013 American Chemical Society. (b) Synthesis of chemical receptor for cyclochexanone: (i) 2-bromoethylamine hydrobromide, DIPEA, 77%; (ii) KSAc, NaI, 27%; (iii) NaOMe, 28%.

response than receptors like bulk polymer coatings, albeit at the expense of dynamic range due to the limited surface area. [28], [29] Self-assembled monolayers are solution-processable, which makes them low-cost and easy to fabricate in comparison to other functionalizing receptors. [30]

Previous work using bulk acoustic wave resonators to sense VOCs has taken advantage of many of these sensitizers. [31]–[39] Of these, only Chang et al. used self-assembled monolayers as the functionalizing material. [34] In that work, the authors used multiple devices with nine different self-assembled monolayers to create an e-nose system that could sense and identify multiple VOCs. This work focuses on characterizing the selectivity and sorption and desorption kinetics of the self-assembled monolayer rather than the individual sensitivity of each self-assembled monolayer/bulk acoustic resonator pair. The large MHz-scale frequency shifts observed do indicate a high sensitivity which emphasizes the advantage of using self-assembled monolayers and bulk acoustic resonators together for VOC sensing.

In this work, the reported capture unit from Frazier et al., which was designed for a carbon nanotube chemiresistor, is chemically modified to integrate with a bulk acoustic wave sensor. [9] This approach allows for a superior demonstrated limit of detection (5 ppm vs. 1.11 ppm), and a straightforward pathway to multi-site integration with other vapor targets in the future.

II. SENSING MECHANISM

In gravimetric sensing schemes, additional mass collected on the surface of a resonator causes a shift in the resonant frequency, which, assuming the negligible effects from non-piezoelectric layers, can described by $\Delta f/\Delta m = -\frac{2f_0^2}{\rho_r V_r}$ where f_0 is the resonant frequency and ρ_r and V_r are the density and acoustic velocity of the piezoelectric material. [40] Even in the most general derivation from Windqvist et al. for the mass sensitivity of a bulk acoustic resonator, the sensitivity $\frac{\partial f}{\partial m}$ increases with the square of the resonant frequency, lending additional sensing advantage to higher frequency resonator structures.

By adding a functional recognition element to the resonator, the affinity of the surface as well as the specificity of the system can be increased so that the sensor performance can be tuned to targeted applications. [41]–[43] With a selective coating, a change in the resonator's frequency can assessed to confirm the presence and concentration of a specific VOC.

The selector used in this work is a trifunctional sensor that creates a self-assembled monolayer (SAM). Its head group is a thiol, which forms a bond with the gold ions on the surface of the bulk acoustic resonator. [44], [45] The functional group of the selector has a thiourea and bis(trifluoromethyl) aryl group. The thiourea group defines the selectivity of the overall molecule. It binds to ketones by forming two hydrogen bonds, as shown in Fig 1a. The bis(trifluoromethyl) aryl group interfaces with the external environment. This group is known to have a strong electron pull, which has been proven to improve the selectivity of thiourea receptors due to improved hydrogen (proton) acidity. [9]

III. DEVICE DESIGN AND FABRICATION

A. Selector Synthesis

All chemicals and reagents were purchased from Sigma-Aldrich (St. Louis, USA) and used without further purification unless noted otherwise. Anhydrous solvents were prepared by filtration through drying columns (Innovative Technology, inc.; Pure Solv): anhydrous dichloromethane (DCM), acetone 3,5-bis(trifluoromethyl)phenyl isothiocyanate (98%), 2-bromoethylamine hydrobromide (99%), diisopropylethylamin (purified by redistillation, DIPEA, 99.5%), potassium thioacetate (98%), sodium iodide (99.5%), sodium sulfate anhydrous (99%), acetone (absolute, 99.5%), sodium methoxide (99.5%). Column chromatography was performed on silica 60 (Merck, 40-63 mm). NMR spectra were recorded on a Bruker Avance DRX-400 spectrometer or a Bruker Avance 200 spectrometer.

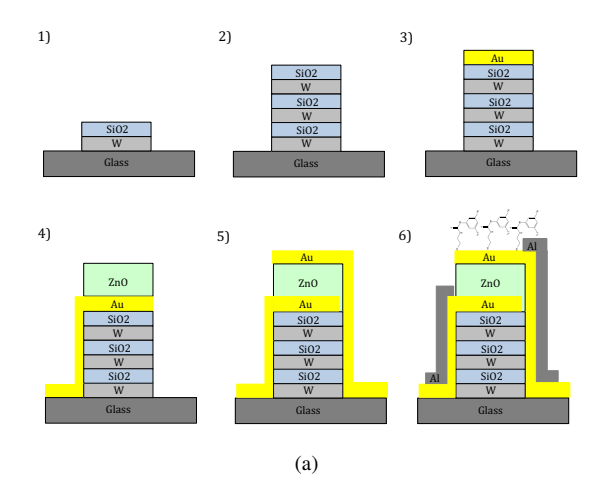
A modified literature procedure was used for the synthesis 1 (1-(3,5-bis(trifluoromethyl)phenyl)-3-(2bromoethyl)thiourea). [9] Under argon atmosphere DIPEA (180 mg, 1.39 mmol, 1.25 eq) was added to a suspension of 2bromoethylamine hydrobromide (227 mg, 1.11 mmol, 1.00 eq) in anhydrous dichloromethane (37 mL) at room temperature and the mixture was stirred until a clear solution was obtained (30 minutes). Then 3,5-bis(trifluoromethyl)phenyl isothiocyanate (300 mg, 1.11 mmol, 1.00 eq) was added slowly dropwise to a stirred solution of 2-bromoethylamine hydrobromide (227 mg, 1.11 mmol, 1.00 eq). The mixture was stirred overnight and then the solvent was removed under reduced pressure. The crude product was washed multiple times with hexane and water and dried in vacuo to yield a white solid. Recrystallization from DCM yielded 1 as white needle-like crystals arranged in dendrite circular structures (343 mg, 77%).

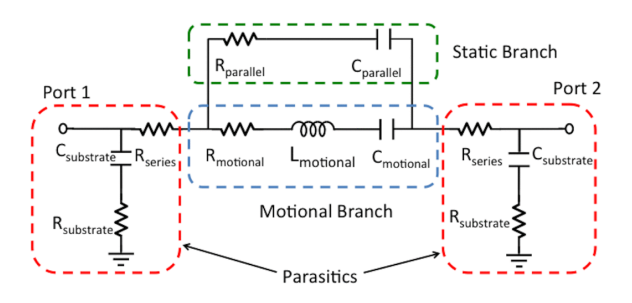
Under argon atmosphere in a 10 ml sealed vial 1 (112 mg, 0.283 mmol, 1.00 eq) was mixed with potassium thioacetate (100 mg, 0.876 mmol, 3.00 eq) and sodium iodide (84 mg, 0.560 mmol, 2.00 eq) in dry acetone (5 ml). The reaction mixture was heated for 3h in a microwave oven at 90°C (50 W). The resulting dark brown mixture was filtered through a 200 μ m syringe filter, washed with DCM and water and dried over anhydrous sodium sulfate. The solvent was removed under reduced pressure to yield a yellow crude oil. The crude oil was then dissolved in hexanes/EtOAc=4:1 and purified via chromatography on silica (hexanes/EtOAc=3:2) to yield **2**(S-(2-(3-(3,5-bis(trifluoromethyl)phenyl)thioureido)ethyl) ethanethioate) as a colorless oil (30 mg, 27%). Following a modified procedure from Liras et al. under argon atmosphere 2 (30 mg, 0.077 mmol, 1.00 eq), an excess of sodium methoxide (50 mg, 0.925 mmol, 12 eq) was added to anhydrous DCM (4 ml) and stirred overnight at room temperature. [46] The solvent was removed under reduced pressure and the crude product was purified via column chromatography (hexanes/EtOAc=3:2) to yield 3 (1-(3,5bis(trifluoromethyl)phenyl)-3-(2-mercaptoethyl)thiourea, mg, 28%).

B. Solidly Mounted Resonator Design

The solidly mounted resonator (SMR) device that serves as the basis for the sensing scheme consists of two major parts: a Bragg reflector and a piezoelectric sandwich. The Bragg reflector acoustically isolates the resonance in the piezoelectric layer from the substrate below and in this case, consists of alternating tuned layers of sputtered silicon dioxide and tungsten. [47] The Bragg mirror can be modeled simply using the acoustic velocity of the high and low impedance materials, and from this model the thickness of each layer can be determined. [48]–[53] Using a MATLAB model, it was determined that three bilayers of tungsten and silicon dioxide (650 nm and 680 nm thick respectively) would provide a Bragg mirror with 99.99 % reflectance at the designed resonator frequency (2 GHz). [54]

As mentioned in the introduction, a resonator with a high resonant frequency and high quality factor will demonstrate higher sensitivity when used as a gravimetric sensor. A Bragg mirror with high reflectance will help ensure a high quality factor, but the piezoelectric material choice and quality will in part determine the quality factor and resonant frequency of the device. The piezoelectric layer chosen for this experiment is c-axis oriented zinc oxide because its high crystallinity yields high quality factors. [55] The frequency of the resonance is defined by $f = v_p/(2t)$ where f, v_p , and t are the resonant frequency, acoustic velocity of piezoelectric material, and thickness of the piezoelectric layer. Using previous literature values for the acoustic velocity of zinc oxide, a 1.3 μ m thick layer of zinc oxide will result in a 2GHz resonant frequency. [54], [56], [57] The piezoelectric layer is contacted with gold electrodes and that contact is reinforced with a thick aluminum layer at the end of processing. The thick aluminum layer is only added along the sidewalls of the Bragg mirror





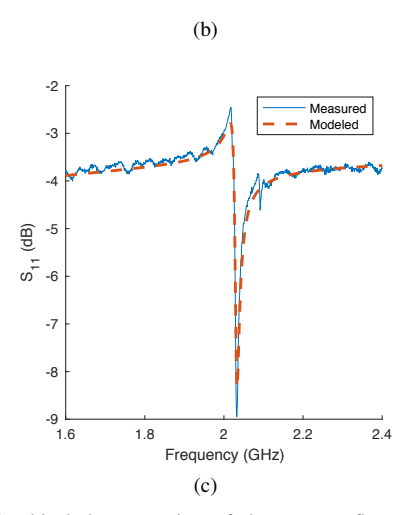


Fig. 2. (a) Graphical demonstration of the process flow used to created solidly mounted resonators: 1-2 Bragg reflector, 3-5 piezoelectric material and electrodes, 6 electrical contact and addition of SAMS (b) Schematic of Butterworth-Van Dyke circuit model (c) Frequency response (S_{11} response) showing resonance of completed devices at 2.03 GHz

to reduce contact resistance and ensure that the contact is not broken between the bonding pads and the piezoelectric layer. The SMR devices are have full dimensions of 400 μm by 500 μm with an active area of 100 μm by 100 μm

C. Solidly Mounted Resonator Fabrication

First, the substrate (50x50x0.7 mm glass slides obtained from LumTec, New Taipei City, Taiwan) is patterned for liftoff with a bilayer resist (LOR30B, MicroChem, Westborough, MA, USA and S1811, Shipley, Marlborough, MA, USA) before sputtering chrome (2" Chrome target, 99.95% 2" dia x 0.250" thick, Kurt J Lesker, Jefferson Hills, PA, USA) and then tungsten (2" Tungsten target, 99.95% 2" dia x 0.250" thick, Kurt J Lesker, Jefferson Hills, PA, USA) under vacuum using an AJA Orion-3 sputterer for a final thickness of 10 nm chrome and 650 nm tungsten. Again using liftoff, 680 nm of silicon dioxide is deposited by AJA Orion-8 RF sputtering (2" SiO2 target, 99.995% 2" dia x 0.125" thick, AJA International, Scituate, MA, USA). These two layers are repeated twice more by patterning and lifting off each time until the final layer of silicon dioxide which is not patterned. Next, a thin chrome adhesion layer (5 nm) and gold contact (100 nm) are deposited using e-beam evaporation in an Angstrom Ultra High Vacuum Evaporator (Angstrom Engineering, Kitchener, Canada) and liftoff using Remover PG (MicroChem, Westborough, MA, USA) heated to 65 C. The 1.2 micron piezoelectric layer (2" ZnO target, 99.99% 2" dia x 0.125" thick, AJA International, Scituate, MA, USA) is deposited by RF sputtering (AJA Orion-8 sputterer) and lifted off as well. Another gold contact is then added via e-beam evaporation before a final thick (1-2 um) layer of sputtered aluminum (2" Aluminum target, 99.95% 2" dia x 0.250" thick, Kurt J Lesker, Jefferson Hills, PA, USA) is used to cover any large steps in the contact path and ensure good contact when probing. At this point, the bare SMR devices were tested for their frequency response, which is shown in Fig. 2c. The measured resonant frequency of the devices and quality factor is 2.03 GHz and 630.4, respectively. After measuring the response, the equivalent circuit model for the device was modelled using the Butterworth-Van Dyke circuit model and determined to have the following Z-parameters: $L_m = 317.749 \text{ nH}, \ R_m = 6.42885\Omega, \ C_m = 19.555 \text{ fF}, \\ C_p = 1649.64 \text{ fF}, \ R_s = 33.1\Omega, \text{ and } R_p = 13.0992\Omega. \ [58]$ The Butterworth-Van Dyke circuit model is shown in Fig. 2b.

Before the chemical receptor can be added, the sample was diced using a Disco DAD 3220 Dicing Saw leaving pieces containing one device each. Each device had dimensions of 400 μ m by 500 μ m with an active area of 100 μ m by 100 μ m. The chemical selector treatment was preceded by a short UV ozone treatment using a UVFAB UV Ozone Cleaner to activate the surface of the glass and increase its reactivity by increasing oxygen dangling bonds on the surface.

A 1 mM solution of the chemical sensor in anhydrous ethanol (Sigma Aldrich, St. Louis, USA) was prepared and the samples were incubated for one hour to allow the self assembling monolayer to attach to the gold electrodes. The sample was then rinsed with ethanol to remove any material excess and dried in nitrogen gas. X-ray photon spectroscopy (XPS) was conducted using a PHI Quantera II Scanning XPS to ensure the presence of selector 3 on the surface of the SMR device. Figure 3a shows a survey scan and Figure 3b a detailed look at the 692-685 eV region, demonstrating the presence of

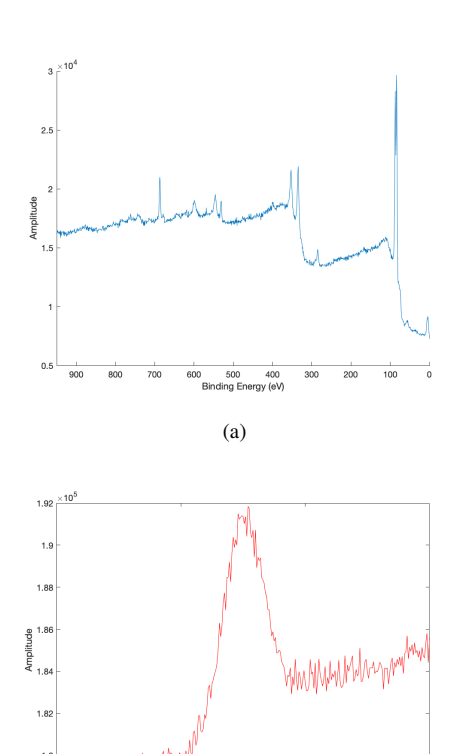


Fig. 3. (a) Wide range XPS scan done to ensure presence of SAM on surface of SMR device. (b) Focused scan to show presence of Fluorine peak indicating the successful adhesion of the SAM to the SMR device.

(b)

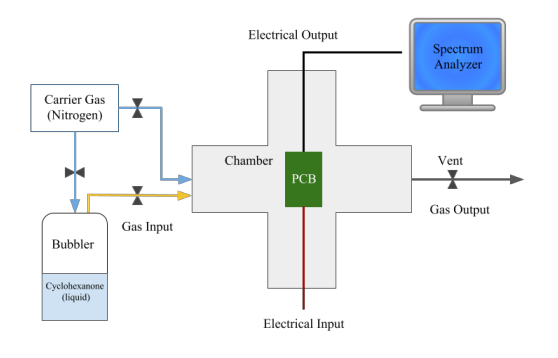
fluorine, and thus indicating a successful functionalization of the selector on the surface.

IV. SYSTEM DESIGN

A. Printed Circuit Board Design

For sensing experiments, an untreated reference device and a treated sensing device were wirebonded to a printed circuit board shown in Fig. 4b. The incorporation of the printed circuit board aims to help mitigate unwanted frequency drifting, or constant downshift, which could obscure the sensor response. The effect of even minute temperature changes on the resonant frequency of bulk acoustic resonators has been well documented. [59]–[62] By mixing the frequency response of the reference and treated devices, temperaturebased drifting will be removed from the final output which is read out by the frequency analyzer. Changes in humidity can also have a similar effect on the devices as water molecules accumulate on the surface and cause unwanted frequency shifts. [63] This problem, however, is not specific to water, and nonspecific binding of other VOCs can present the same source of error in sensing. [?] The two devices experience the same environment on the printed circuit board, and simultaneously observing the responses of the reference device will help remove any erroneous shifting due to these environmental changes.

The printed circuit board has two radio frequency (RF) oscillators using HEMTs (ATP34143 GaAs JFET) and RF



PCB Power (USB)

Unitreated Resonator

Frequency Differential Resonator

Filters and Mixer

(a)

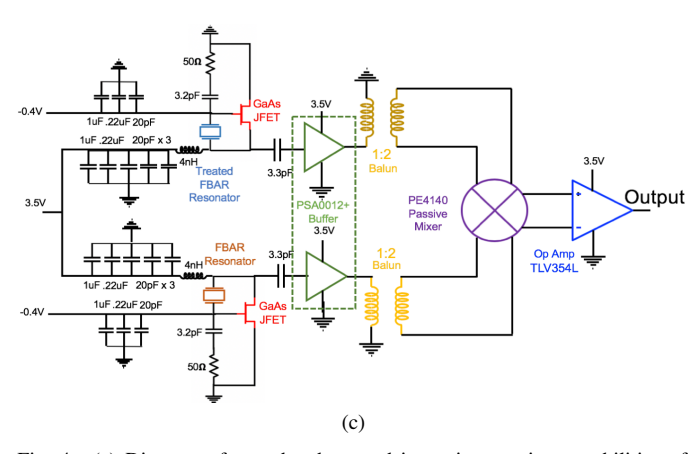


Fig. 4. (a) Diagram of gas chamber used in testing sensing capabilities of SMR devices using a bubbler to vaporize cyclohexanone before it is mixed with a carrier gas for dilution. Two electrical feedthroughs provided power via USB and the high frequency connection was transmitted via an SMA connector and coaxial cable. (b) Image of PCB with boxes highlighting attached devices. USB input was used to power the devices and an SMA output was used to read out frequency differential resulting from filters and mixer. (c) Detailed schematic of PCB.

buffers (mini-circuits PSA0012+), the core of the oscillators were solidly mounted resonators on glass wire bonded to the board. The outputs of the oscillators then go to a mixer (pSemi Quad Mixer PE4140) and op amp (TLV354L) to eliminate common noise and drift. The PCB was designed to operate at a GHz frequency and was modeled and simulated with transmission lines in Advanced Design Software (ADS). A USB port was used for biasing the devices. The board's SMA port gave the output signal readout which was connected to a spectrum analyzer which recorded frequency data.

The SMR devices themselves typically require very little power, so the power requirements of the PCB is the limiting factor in the total amount of power required for the sensor. Previous work by our group shows that the designed solidly mounted resonator draws 9.9 mW of power. [54] Other works have shown that solidly mounted resonators can draw as little as 0.3 mW. [?] In this work, the transistor for the oscillator was biased around 3.5V on the drain and -0.4 V on the gate which draws 60 mA of current. The buffer of the oscillator is also biased at 3.5V drawing 24mA. Finally, the output amplifier, also biased at 3.5V, draw 2.5mA which is a total power consumption of 371.25 mW. This is comparable to work by Nimal et al. where a similar handheld device was shown to draw low power of approximately 300 mW. [64] Everything else including the mixer are passive and do not draw any current. To improve the PCB for low-power applications, higher quality components and a high frequency PCB material could be used to reduce parasitics. In order to drastically decrease the system's power needs, the PCB circuit would need to be adapted to CMOS. The small transistor size then can be leveraged to minimize the required power. Previous work with a monolithically integrated bulk acoustic wave resonator shows power draw of approximately 4-60 mW for the system. [54], [65], [66]

With the devices wirebonded to the PCB, the entire sensing device then is contained in the dimensions of the PCB, which are 4.18 cm by 7.96 cm. In similarly-sized handheld devices discussed by Nimal et al., the acoustic resonators used were significantly larger than the devices used in our devices. [64] In comparison to many of the large, table-top systems which are commonly used for gas sensing like GC-MS, these handheld devices are significantly smaller and more portable. The necessity of a spectrum analyzer at this stage of the development does hamper the portability, but as mentioned previously, the current PCB design could be adapted to CMOS to further reduce the size of the system. The overall performance and computing power of CMOS would also likely facilitate the removal of the spectrum analyzer from the system.

V. TESTING CHAMBER DESIGN

A chamber was built for dynamic flow testing the SAMs on SMR and their sensitivity to different VOCs. Acetone (99.5 %, Fischer Scientific, Fair Lawn, NJ, USA), toluene (anhydrous, 99.8 %, Sigma Aldrich, St. Louis, USA), and cyclohexanone (reagant grade, 99.8 %, Sigma Aldrich, St. Louis, USA) were used to test cross-sensitivity and responsivity of devices. The chamber is a 4-way stainless steel QF flange cross that allows for rapid part exchange. Two inputs were designated for electrical feedthroughs and read outs and the remaining two for gas flow and exhaust. The electrical feedthroughs were used for the USB and SMA ports of the PCB. There are two gas input lines, one for pure nitrogen gas flow for dilution and the other one is for the VOC flow. The VOC was converted from its liquid form to a saturated room temperature vapor using a bubbler and then mixed with the carrier gas, dry nitrogen, before entering the gas chamber. The resonant frequency differential between the two sites was observed by a spectrum analyzer (Agilent E440A, Santa Clara, CA, USA). A schematic and image of the system and printed circuit board with devices can be seen in Fig. 4. All tests were performed at room temperature and pressure.

VI. SENSOR CHARACTERIZATION

A. Sensitivity for Cyclohexanone

To test the sensitivity of the coating the sensor was exposed to cyclohexanone in concentrations ranging from 3.8 to 50 ppm. To ensure equilibrium conditions the chamber was flushed with nitrogen for two minutes before the measurements were started. Cyclohexanone of different concentrations was flushed into the chamber for approximately two minutes to allow ensure again steady conditions. Then cyclohexanone flow was turned off and pure nitrogen was used to purge the chamber again for three minutes to remove cyclohexanone and allow the system to return to baseline. The limit of detection (LOD) was extracted by plotting the sensors maximum response to the varying concentrations and fitting the data.

The VOC concentration was calculated using the equation:

$$C_{ppm} = \left(\frac{P_s}{P} \times \frac{F_{VOC}}{F_{VOC} + F}\right) \times 10^6 \tag{1}$$

where P_s is the saturated partial pressure in mm Hg, P is the chamber pressure (760 mmHg), F_{VOC} is the flow in sccm of the VOC, and F is the carrier gas (N_2) flow in sccm. [67] Antoine's equation

$$\log_{10}(P) = A - \frac{B}{T + C} \tag{2}$$

was used to calculate the partial pressure in the gas chamber where $A,\,B,\,$ and C are unitless constants known as Antoine's constants and T is the temperature in Kelvin. For cyclohexanone, Antoine's constants are

$$A = 4.1033 \pm 0.00099 \tag{3}$$

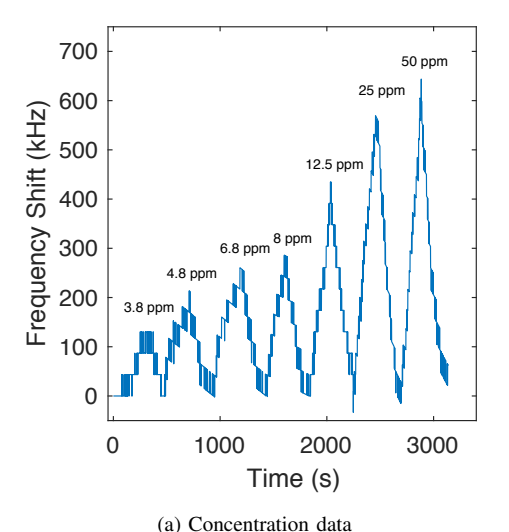
$$B = 1495.51 \pm 0.67 \tag{4}$$

$$C = -63.598 \pm 0.075 \tag{5}$$

for room temperature. [68]

The resulting frequency shifts of the concentration detection measurements are shown in Fig. 5a. For low concentrations, the shifts are approximately linear but this trend breaks for higher concentrations. There are several possible explanations of this trend. It is more likely that as the concentration is increased, the SAM receptor sites became completely filled. Once the sites have become filled, the response will no longer track linearly with concentration and begin to flatten, as seen in the data above 12.5 ppm. Otherwise, the surface coverage and chemical stability of the monolayer could account for the nonlinearity but will need to be investigated further. Experimentally, it is possible that a longer time at equilibrium may help extend the linearity to higher concentrations, but as the device does return to equilibrium after each sensing, this source of experimental error is unlikely to be the sole contributor to the nonlinearity at higher concentrations. However, higher concentration still leads to a larger frequency shift which is a good indication for successful cyclohexanone sensing. The extracted sensitivity from this experiment for explosive detection at low concentrations is approximately 39 kHz/ppm.

From this data, the noise floor was extracted from the BSL deviation to be 14kHz. [69] When the signal-to-noise ratio (SNR) is approximately 3 the signal is pure, so this is the criterion used to determine the LOD. [70] The extracted LOD is shown in Fig. 5b to be 1.11ppm, lower than the previous demonstrator of the thiourea monolayer for cyclohexanone detection. [9] Similar functionalized bulk acoustic wave sensors have shown limits of detection between 500 and 4 ppm, so a limit of detection of 1.11 ppm is competitive. [34], [36], [38], [39], [41]



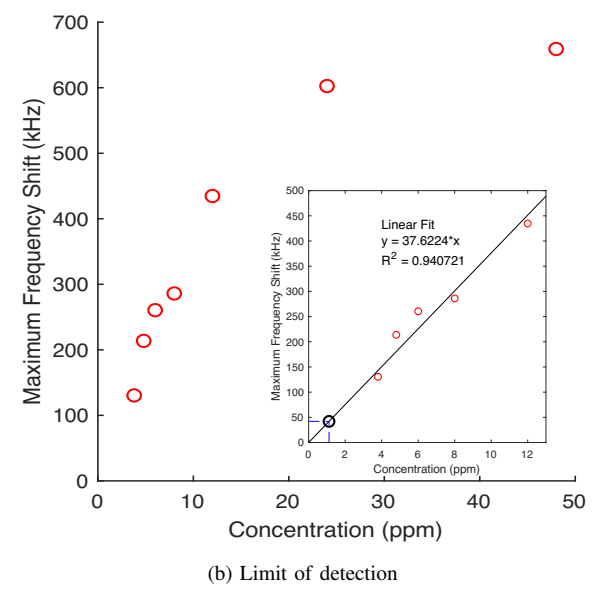


Fig. 5. (a)Result of concentration detection experiment where sensor was exposed to cyclohexanone which was diluted with nitrogen to concentrations from 3.8 to 50 ppm (b) Extrapolation of limit of detection via concentration detection data shown in Fig. 5a

B. Selectivity for Cyclohexanone

To determine the selectivity of the sensor and validate the role of the selector three separate VOCS were tested with-

Analyte	Min. Concentration (ppm)	Sensitvity (kHz/ppm)
Acetone	44151	0.014
Toluene	5588	0.107
Cyclohexanone	890	1.210

TABLE I

FREQUENCY RESPONSE OBSERVED FOR VARYING CONCENTRATIONS OF CYCLOHEXANONE, ACETONE, AND TOLUENE. THESE RESULTS DEMONSTRATE APPROXIMATELY THE SAME RELATIVE RESPONSE AND SELECTIVITY AS WAS MEASURED USING A RESISTIVE APPROACH FOR THE SAME RECEPTOR IN PREVIOUS WORK. [71]

out dilution: acetone, toluene, and cyclohexanone. The same chamber is used as in previous measurements but different equations will govern the concentration of the VOC due to the lack of dilution. To calculate the concentration in the chamber for each VOC the volume of the chamber was calculated, and the VOC concentration in parts per million was extracted by time and flow as follows,

$$C_{ppm} = \frac{V_{VOC}}{V_{chamber}} = \frac{f_{VOC}t_{flow}}{V_{chamber}}$$
 (6)

where V_{VOC} is the VOC volume in the chamber, $V_{chamber}$ is the chamber volume (both volumes are in cm^3), f_{VOC} is the VOC flow into the chamber and t_{flow} is the time the VOC was flowing into the chamber in minutes. The minimum concentrations used for cyclohexanone, acetone and toluene are 890ppm, 44151ppm and 5588ppm, respectively. The concentration of each analyte was increased in every cycle, and each cycle consisted of five minutes of analyte followed by five minutes of relaxation time with an inflow of nitrogen. The resulting responses, normalized for concentration changes between analytes, have been added in Fig. 6. The results are also summarized in Table I.

Cyclohexanone consistently generated a frequency shift two to five times greater than that of either toluene or acetone despite its concentration in all cases being over five times less than the other analytes. Additionally, the acetone and toluene reactions do not scale with concentration, instead showing saturation and flattening which implies the molecules are covering the surface but not reacting with the selector. Since the sensitivity of the selector to acetone and toluene is ten to a hundred times higher, we could expect that the point of saturation for these molecules would occur at concentrations ten to a hundred times higher than that of cyclohexanone. However, the almost identical responses to varying concentrations under these thresholds indicate that saturation has already occurred, which would not happen if the acetone and toluene were actually reacting with and binding to the selector. Instead, the acetone and toluene cover the surface haphazardly, which happens at all concentrations, and causes an almost identical frequency shift. The high response magnitude and responsivity to concentration changes shows that the monolayer attached to the device has a high selectivity for cyclohexanone.

C. Reference and Repeatability

To ensure the sample's response was coming from the coating's sensing capabilities another PCB was prepared with two uncoated samples and placed in the chamber. In

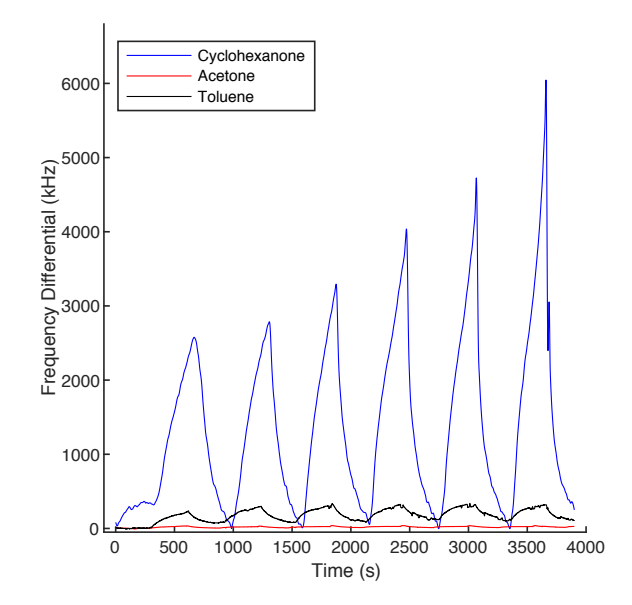


Fig. 6. Normalized real-time frequency response of sensor to increasing concentrations of cyclohexanone, toluene, and acetone

Fig. 7, the VOC flow was on for three minutes with no measurable change in the frequency differential, indicating that the measured responses are a result of the monolayer binding to cyclohexanone.

To prove that the sensing is repeatable, several

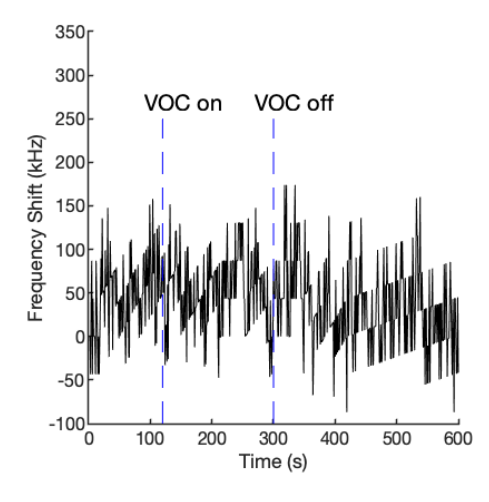


Fig. 7. Frequency response of devices without cyclohexanone selective coating when exposed to cyclohexanone which indicate selector

measurements were taken with the same concentration of cyclohexanone. In Fig. 8, the sensor was tested with 50 ppm of cyclohexanone and left for 4 minutes to ensure steady state conditions before being flushed again with pure nitrogen. After three minutes, cyclohexanone was turned back on and this process repeated twice more. The repeatability measurement shows responses within 4% of the mean shift when the device is exposed to the same concentration, which indicates a very reproducible measurement. Long-term stability should be investigated further, but the device was used for over a month with no observable diminishing

of response. The solution containing the SAMS was used reliably in fabrication and testing over several months, and similar SAMs have shown no change in performance after a month, indicating long term stability of at least a few months. [72]

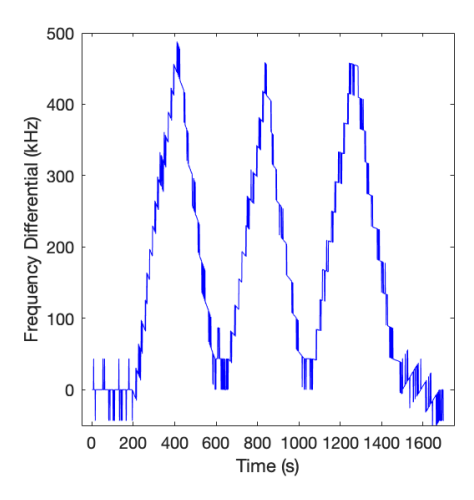


Fig. 8. Frequency response to repeated exposure to same concentration of cyclohexanone (50 ppm) observed to indicate repeatability of sensor measurements.

While the printed circuit board was designed with a reference device to eliminate the influence of humidity and temperature fluctuations on the devices, the system still demonstrated some drift which was likely due to humidity and temperature fluctuations. Humidity can cause unwanted frequency drift as the water molecules can sit on the surface of the devices and mimic the mass loading involved in sensing. [63] Temperature changes can also lead to unwanted frequency shifts as the resonance of zinc oxide can be affected by temperature changes. [59], [60] Adding pressure and temperature monitoring might simplify future testing and allow for a lower LOD. With optimization of the gas lines and monitoring the chamber parameters the response time could also be improved. Additionally, the recovery times are relatively slow (> 5 minutes), often much longer than the time to maximum response (< 3minutes), which would not be ideal for real-time applications. However, for threat detection, the fast response time is much more critical than recovery time.

Despite these challenges, this technology (at the mm-scale) is significantly smaller and less expensive than gas chromatography and mass spectrometry systems, which makes it ideal for real-time monitoring [12]. The solidly mounted resonators used in this work have a much higher resonant frequency than most quartz crystal monitors which leads to a much higher sensitivity (39 kHz/ppm) than those sensors (2 Hz/ppm) [25]. Integration of a sensing and control device to a printed circuit board eliminates some of the frequency drifting that plagues quartz crystal monitor based sensors [73]. Finally, the limit of detection demonstrated here (1.11 ppm) is the lowest demonstrated for cyclohexanone among comparable chemiresistor and MEMs devices [9], [20], [25], [26], [39]. In particular, Heil et al and Zeng et al used gravimetric

approaches resulting in limits of detection for cyclohexanone of 5 and 40 pppm respectively so our demonstration of 1.11 ppm is a significant improvement on this previous work. This approach can also be scaled to an array with bulk acoustic wave resonators functionalized for different analytes for artificial nose applications [74].

VII. CONCLUSION

Successful integration of a functional self assembled monolayer designed to detect cyclohexanone with a bulk acoustic wave resonator has been demonstrated and the resulting devices have shown reproducible and highly sensitive measurements. The limit of detection demonstrated is 1.11 ppm, which is lower than previously demonstrated using a similar receptor and a chemiresistive readout. This approach unlocks a significant opportunity to use chemical receptors previously burdened with electrical and optical functionalities in new resonator-based detectors with exceptionally low cost, size, and power requirements.

ACKNOWLEDGMENT

The authors thank the staff of the City College of New York Advanced Science Research Center and the Clean Room Columbia Nano Initiative Clean Room, especially Dr. Jaeeun Yu. The authors gratefully acknowledge funding from the National Science Foundation Graduate Research Fellowship Program grant number DGE - 1644869 and ECCS programs 1343282 and 1641100. Support through the doctoral program (TUW) *Unraveling advanced 2D materials* is gratefully acknowledged. The authors also thank Dr. Daniel Paley for XPS measurements.

REFERENCES

- [1] M. J. A. K. Brown, M. R. Sim and C. N. Gray, "Concentrations of volatile organic compounds in indoor air - a review," *Indoor Air*, vol. 4, no. 2, pp. 123–124, 1994.
- [2] B. Szulczyński and J. Gebicki, "Currently commercially available chemical sensors employed for detection of volatile organic compounds in outdoor and indoor air," *Environments*, vol. 4, no. 1, p. 21, 2017.
- [3] J. Kesselmeier and M. Staudt, "Biogenic volatile organic compunds (voc): An overview on emission, physiology and ecology," *J. Atmos. Chem.*, vol. 33, pp. 23–88, 1999.
- [4] A. Guenther, C. N. Hewitt, D. Erickson, R. Fall, C. Geron, T. Graedel, P. Harley, L. Klinger, M. Lerdau, W. A. Mckay, T. Pierce, B. Scholes, R. Steinbrecher, R. Tallamraju, J. Taylor, and P. Zimmerman, "A global model of natural volatile organic compound emissions," *Journal of Geophysical Research: Atmospheres*, vol. 100, no. D5, pp. 8873–8892. [Online]. Available: https://agupubs.onlinelibrary.wiley.com/doi/abs/10.1029/94JD02950
- [5] C. T. Nguyen and R. T. Howe, "An integrated cmos micromechanical resonator high-q oscillator," *IEE J. Solid-State Circuits*, vol. 34, no. 2.
- [6] R. H. J. Bustillo and R. Muller, "Surface micromachining for microelectromechanical systems," *Proc. IEEE*, vol. 86, no. 8.
- [7] W. Miekisch, J. K. Schubert, and G. F. E. Noeldge-schomburg, "Diagnostic potential of breath analysis? focus on volatile organic compounds," *Clinica Chimica Acta*, vol. 347, pp. 25–39, 2004.
- [8] R. P. M. C. I. C. T. F. Jenkins, W. F. O'Reilly, "Detection of cyclohexanone in the atmosphere above emplaced antitank mines," COLD REGIONS RESEARCH AND ENGINEERING LAB, NH, Tech. Rep. AD0778741, Apr. 1974.
- [9] K. M. Frazier and T. M. Swager, "Robust cyclohexanone selective chemiresistors based on single-walled carbon nanotubes," *Anal. Chem.*, vol. 85, no. 15, pp. 7154–7158, 2013.

- [10] S. T. S. Giannoukos, B. Brkić and N. France, "Membrane inlet mass spectrometry for homeland security and forensic applications," *J. Am. Soc. Mass Spectrom.*, vol. 26, no. 2, pp. 231–239, 2015.
- [11] G. G. J. K. A. O. T. H. Ong, T. Mendum and R. Kunz, "Use of mass spectrometric vapor analysis to improve canine explosive detection efficiency," *Anal. Chem.*, vol. 89, no. 12, pp. 6482–6490, 2017.
- [12] C. K. Ho, M. T. Itamura, M. Kelley, and R. C. Hughes, "Review of Chemical Sensors for In-Situ Monitoring of Volatile Contaminants," Sandia National Laboratories, NM, Tech. Rep. SAND2001-0643, Mar. 2001.
- [13] S. Giannoukos, B. Brki, S. Taylor, and N. France, "Membrane Inlet Mass Spectrometry for Homeland Security and Forensic Applications," J. Am. Soc. Mass Spectrom., pp. 231–239, 2015.
- [14] M. Agah, G. R. Lambertus, R. Sacks, and K. Wise, "High-Speed MEMS-Based Gas Chromatography," *Journal of Microelectromechanical Systems*, vol. 15, no. 5, pp. 1371–1378, 2006.
- [15] M. R. Cavallari, G. S. Braga, M. F. P. Silva, J. E. E. Izquierdo, L. G. Paterno, E. A. T. Dirani, I. Kymissis, and F. J. Fonseca, "A Hybrid Electronic Nose and Tongue for the Detection of Ketones: Improved Sensor Orthogonality Using Graphene Oxide-Based Detectors," *IEEE Sensors Journal*, vol. 17, no. 7, pp. 1971–1980, 2017.
- [16] B. Wang, J. C. Cancilla, J. S. Torrecilla, and H. Haick, "Arti fi cial Sensing Intelligence with Silicon Nanowires for Ultraselective Detection in the Gas Phase," NANOLetters, 2014.
- [17] J. M. Schnorr, D. V. D. Zwaag, J. J. Walish, Y. Weizmann, and T. M. Swager, "Sensory Arrays of Covalently Functionalized Single-Walled Carbon Nanotubes for Explosive Detection," *Advanced Functional Materials*, pp. 5285–5291, 2013.
- [18] E. J. Severin, B. J. Doleman, and N. S. Lew, "An Investigation of the Concentration Dependence and Response to Analyte Mixtures of Carbon Black / Insulating Organic Polymer Composite Vapor Detectors," *Anal. Chem.*, vol. 72, no. 4, pp. 658–668, 2000.
- [19] Z. Yang and X. Dou, "Emerging and Future Possible Strategies for Enhancing 1D Inorganic Nanomaterials-Based Electrical Sensors towards Explosives Vapors Detection," *Advanced Functional Materials*, pp. 2406–2425, 2016.
- [20] K. A. Mirica, J. M. Azzarelli, J. G. Weis, J. M. Schnorr, and T. M. Swager, "Rapid prototyping of carbon-based chemiresistive gas sensors on paper," PNAS, vol. 2013, pp. 3265–3270, 2013.
- [21] S. Fanget, S. Hentz, P. Puget, J. Arcamone, M. Matheron, E. Colinet, P. Andreucci, L. Duraffourg, E. Meyers, and M. L. Roukes, "Gas sensors based on gravimetric detection - A review," *Sensors and Actuators, B: Chemical*, vol. 160, no. 1, pp. 804–821, 2011. [Online]. Available: http://dx.doi.org/10.1016/j.snb.2011.08.066
- [22] K. Länge, "Bulk and surface acoustic wave sensor arrays for multianalyte detection: A review," Sensors (Switzerland), vol. 19, no. 24, 2019.
- [23] E. J. Houser, T. E. Mlsna, V. K. Nguyen, R. Chung, R. L. Mowery, and R. A. Mcgill, "Rational materials design of sorbent coatings for explosives: applications with chemical sensors," *Talanta*, vol. 54, pp. 469–485, 2001.
- [24] G. Zuo, X. Li, Z. Zhang, and T. Yang, "Dual-SAM functionalization on integrated cantilevers for specific trace-explosive sensing and nonspecific adsorption suppression," *Nanotechnology*, 2007.
- [25] C. Heil, G. R. Windscheif, J. Florke, J. Glaser, M. Lopez, U. Schramm, J. Bargon, and F. Vogtle, "Highly selective sensor materials for discriminating carbonyl compounds in the gas phase using quartz microbalances," Sensors and Actuators: B, pp. 51–58, 1999.
- [26] J. M. Azzarelli, K. A. Mirica, J. B. Ravnsbæk, and T. M. Swager, "Wireless gas detection with a smartphone via rf communication," *PNAS*, vol. 2014, pp. 1–5, 2014.
- [27] V. M. Mirsky and A. Yatsimirsky, Artificial receptors for chemical sensors. John Wiley & Sons, 2010.
- [28] R. M. C. A. J. Ricco and G. C. Osbourn, "Surface acoustic wave chemical sensor arrays: New chemically sensitive interfaces combined with novel cluster analysis to detect volatile organic compounds and mixtures," Acc. Chem. Res., vol. 31, no. 5, pp. 289–296, 1998.
- [29] R. M. Crooks and A. J. Ricco, "New organic materials suitable for use in chemical sensor arrays," Acc. Chem. Res., vol. 31, no. 5, pp. 219–227, 1998.
- [30] F. Schreiber, "Structure and growth of self-assembling monolayers," Progress in Surface Science, vol. 65, no. 5-8, pp. 151–257, 2000.
- [31] M. Rinaldi, C. Zuniga, and G. Piazza, "SS-DNA functionalized array of ALN Contour-Mode NEMS Resonant Sensors with single CMOS multiplexed oscillator for sub-ppb detection of volatile organic chemicals," in *Proceedings of the IEEE International Conference on Micro Electro Mechanical Systems (MEMS)*, no. Figure 2. IEEE, 2011, pp. 976–979.

- [32] M. L. Johnston, H. Edrees, I. Kymissis, and K. L. Shepard, "Integrated VOC vapor sensing on FBAR-CMOS array," in *Proceedings of the IEEE International Conference on Micro Electro Mechanical Systems* (MEMS), no. February. IEEE, 2012, pp. 846–849.
- [33] Y. Lu, Y. Chang, N. Tang, H. Qu, J. Liu, W. Pang, H. Zhang, D. Zhang, and X. Duan, "Detection of Volatile Organic Compounds Using Microfabricated Resonator Array Functionalized with Supramolecular Monolayers," ACS Applied Materials and Interfaces, vol. 7, no. 32, pp. 17893–17903, 2015.
- [34] Y. Chang, N. Tang, H. Qu, J. Liu, D. Zhang, H. Zhang, W. Pang, and X. Duan, "Detection of Volatile Organic Compounds by Self-assembled Monolayer Coated Sensor Array with Concentration-independent Fingerprints," *Scientific Reports*, vol. 6, no. 23970, pp. 1–12, 2016. [Online]. Available: http://dx.doi.org/10.1038/srep23970
- [35] W. Wang, D. Chen, H. Wang, W. Yu, M. Wu, and L. Yang, "Film bulk acoustic formaldehyde sensor with layer-by-layer assembled carbon nanotubes/polyethyleneimine multilayers," Journal of Physics D: Applied Physics, vol. 51, no. 5, p. 055104, feb 2018. [Online]. Available: http://stacks.iop.org/0022-3727/51/i=5/a=055104?key=crossref.16ff7cde547247c0e6b1f76b6f30ca68
- [36] L. Wang, A. Lin, and E. S. Kim, "Miniature sensing system with FBAR-Based oscillators and frequency shift detector," *IEEE Sensors Journal*, vol. 18, no. 18, pp. 7633–7637, 2018.
- [37] S. Song, D. Chen, H. Wang, Q. Guo, W. Wang, M. Wu, and W. Yu, "Film bulk acoustic formaldehyde sensor with polyethyleneiminemodified single-wall carbon nanotubes as sensitive layer," *Sensors* and Actuators, B: Chemical, vol. 266, pp. 204–212, 2018. [Online]. Available: https://doi.org/10.1016/j.snb.2018.03.129
- [38] Y. Chang, H. Qu, X. Duan, L. Mu, and M. A. Reed, "VOC detection using multimode E-nose composed of bulk acoustic wave resonator and silicon nanowire field effect transistor array," *Proceedings of IEEE Sensors*, vol. 1, no. C, pp. 1–3, 2017.
- [39] G. Zeng, C. Wu, Y. Chang, C. Zhou, B. Chen, M. Zhang, J. Li, X. Duan, Q. Yang, and W. Pang, "Detection and Discrimination of Volatile Organic Compounds using a Single Film Bulk Acoustic Wave Resonator with Temperature Modulation as a Multiparameter Virtual Sensor Array," ACS Sensors, vol. 4, no. 6, pp. 1524–1533, 2019.
- [40] G. Wingqvist, V. Yantchev, and I. Katardjiev, "Mass sensitivity of multilayer thin film resonant BAW sensors," *Sensors and Actuators, A: Physical*, vol. 148, no. 1, pp. 88–95, 2008.
- [41] I. K. M. L. Johnston, H. Edrees and K. L. Shepard, "Integrated voc vapor sensing on fbar-cmos array," in *Proc. IEEE International Conference on Microelectromechanical Systems (MEMS '12)*, Paris, France, Feb. 2012, pp. 846–849.
- [42] Y. Chang, H. Qu, X. Duan, L. Mu, and M. A. Reed, "VOC detection using multimode E-nose composed of bulk acoustic wave resonator and silicon nanowire field effect transistor array," *Proceedings of IEEE Sensors*, vol. 1, no. C, pp. 1–3, 2017.
- [43] N. T. H. Q. W. P. D. Z. H. Z. X. D. Y. Lu, Y. Chang, "Concentration-independent fingerprint library of volatile organic compounds based on gas-surface interactions by self-assembled monolayer functionalized film bulk acoustic resonator arrays," in *Proc. IEEE Sensors*, Busan, South Korea, Nov. 2015, pp. 4–7.
- [44] Y. Xue, X. Li, H. Li, and W. Zhang, "Quantifying thiol-gold interactions towards the efficient strength control," *Nature Communications*, vol. 5, 2014
- [45] Y. Yourdshahyan, H. K. Zhang, and A. M. Rappe, "N -alkyl thiol head-group interactions with the Au(111) surface," *Physical Review B -Condensed Matter and Materials Physics*, vol. 63, no. 8, pp. 1–4, 2001.
- [46] M. Liras, O. Garcia, I. Quijada-Garrido, and R. Paris, "Transformation of the Bromine End Group into Thiol in (Meth)Acrylic Polymers Synthesized by Atom Transfer Radical Polymerization," *Macromolecules*, vol. 44, no. 6, pp. 1335–1339, 2011.
- [47] S. Mahon and R. Aigner, "Bulk Acoustic Wave Devices? Why, How, and Where They are Going (Film Bulk Acoustic Resonator)," CS MANTECH Conference, pp. 15–18, 2007.
- [48] W. E. Newell, "Face-Mounted Piezoelectric Resonators," Proceedings of the IEEE, vol. 53, no. 6, pp. 575–581, 1965.
- [49] M. Lakin, K. T. McCarron, and R. Rose, "Solidly mounted resonators," Proceedings - IEEE Ultrasonics Symposium, pp. 905–908, 1995.
- [50] H. Kobayashi, Y. Ishida, K. Ishikawa, A. Doi, and K. Nakamura, "Fabrication of piezoelectric thin film resonators with acoustic quarterwave multilayers," *Japanese Journal of Applied Physics, Part 1: Regular Papers and Short Notes and Review Papers*, vol. 41, no. 5 B, pp. 3455–3457, 2002.

- [51] S. Salgar, G. Kim, D. H. Han, and B. Kim, "Modeling and simulation of the thin film bulk acoustic resonator," *Proceedings of the Annual IEEE International Frequency Control Symposium*, pp. 40–44, 2002.
- [52] S. Marksteiner, J. Kaitila, G. G. Fattinger, and R. Aigner, "Optimization of acoustic mirrors for solidly mounted BAW resonators," *Proceedings* - *IEEE Ultrasonics Symposium*, vol. 1, no. c, pp. 329–332, 2005.
- [53] S. Jose, R. Hueting, and A. Jansman, "Modelling of bulk acoustic wave resonators for microwave filters," 11th Annual Workshop on Semiconductor Advances for Future Electronics and Sensors, SAFE 2008, vol. 1, pp. 558–561, 2008.
- [54] H. M. Edrees, A. R. Colón-Berrios, D. De Godoy Peixoto, K. L. Shepard, P. R. Kinget, and I. Kymissis, "Monolithically Integrated CMOS-SMR Oscillator in 65 nm CMOS Using Custom MPW Die-Level Fabrication Process," *Journal of Microelectromechanical Systems*, vol. 26, no. 4, pp. 846–858, 2017.
- [55] Y. H. Hsu, J. Lin, and W. C. Tang, "RF sputtered piezoelectric zinc oxide thin film for transducer applications," *Journal of Materials Science: Materials in Electronics*, vol. 19, no. 7, pp. 653–661, 2008.
- [56] G. N. Saddik, J. Son, S. Stemmer, and R. A. York, "Improvement of barium strontium titanate solidly mounted resonator quality factor by reduction in electrode surface roughness," *Journal of Applied Physics*, vol. 109, no. 9, pp. 1–4, 2011.
- [57] A. Vorobiev, J. Berge, S. Gevorgian, M. Löffler, and E. Olsson, "Effect of interface roughness on acoustic loss in tunable thin film bulk acoustic wave resonators," *Journal of Applied Physics*, vol. 110, no. 2, 2011.
- [58] J. D. Larson, P. D. Bradley, S. Wartenberg, and R. C. Ruby, "Modified Butterworth-Van Dyke circuit for FBAR resonators and automated measurement system," *Proceedings of the IEEE Ultrasonics Symposium*, vol. 1, pp. 863–868, 2000.
- [59] E. H. M. C. C. M. R. Colon Berrios, Aida R and I. Kymissis, "CMOS Integrated ZnO Thin Film Bulk Acoustic Resonator with Si3N4 Susceptor Layer for Improved IR Sensitivity," 2017 75th Annual Device Research Conference (DRC), 2017.
- [60] K. T. M. K. M. Lakin and J. F. McDonald, "Temperature compensated bulk acoustic thin film resonators," 2000 IEEE Ultrasonics Symposium. Proceedings. An International Symposium (Cat. No.00CH37121), vol. 1, pp. 855–858 vol.1, 2000.
- [61] S. Ohta, K. Nakamura, A. Doi, and Y. Ishida, "Temperature Characteristics of Solidly Mounted Piezoelectric Thin Film Resonators 2003 IEEE ULTRASONICS SYMPOSIUM-2011 2003 IEEE ULTRASONICS SYMPOSIUM-2012," in *IEEE Symposium on Ultrasonics*. IEEE, 2003.
- [62] K. Bodenhöfer, A. Hierlemann, G. Noetzel, U. Weimar, and W. Göpel, "Performances of mass-sensitive devices for gas sensing: Thickness shear mode and surface acoustic wave transducers," *Analytical Chemistry*, vol. 68, no. 13, pp. 2210–2218, 1996.
- [63] T. R. Z. J. O. J. Y. C. W. Z. Y. H. Qiu, Xiaotun, "Experiment and theoretical analysis of relative humidity sensor based on film bulk acoustic-wave resonator," *Sensors and Actuators, B: Chemical*, vol. 147, pp. 381–384, 2010.
- [64] A. T. Nimal, U. Mittal, M. Singh, M. Khaneja, G. K. Kannan, J. C. Kapoor, V. Dubey, P. K. Gutch, G. Lal, K. D. Vyas, and D. C. Gupta, "Development of handheld SAW vapor sensors for explosives and CW agents," Sensors and Actuators, B: Chemical, vol. 135, no. 2, pp. 399–410, 2009.
- [65] K. B. Östman, S. T. Sipilä, I. S. Uzunov, and N. T. Tchamov, "Novel VCO architecture using series above-IC FBAR and parallel LC resonance," *IEEE Journal of Solid-State Circuits*, vol. 41, no. 10, pp. 2248– 2256, 2006.
- [66] M. Aissi, E. Tourniez, M. A. Dubois, G. Parat, and R. Plana, "A 5.4GHz 0.35μm BiCMOS FBAR resonator oscillator in above-IC technology," Digest of Technical Papers IEEE International Solid-State Circuits Conference, vol. 2, no. 3, pp. 1228–1235, 2006.
- [67] H. Nguyen and S. A. El-Safty, "Meso- and macroporous Co3O4 nanorods for effective VOC gas sensors," *Journal of Physical Chemistry C*, vol. 115, no. 17, pp. 8466–8474, 2011.
- [68] E. F. Meyer and R. D. Hotz, "High-Precision Vapor-Pressure Data for Eight Organic Compounds," *Journal of Chemical and Engineering Data*, vol. 18, no. 4, pp. 359–362, 1973.
- [69] Q. Y. M. C. J. H. J. Li, Y. Lu and M. Meyyappan, "Carbon nanotube sensors for gas and organic vapor detection," *Nano Lett.*, vol. 3, no. 7, pp. 929–933, 2003.
- [70] L. A. Currie, "Nomenclature in evaluation of analytical methods, including detect ion and quantification capa bi i it ies," *Pure Chem Appl.*, vol. 67, no. 10, pp. 1699–1723, 1995.
- [71] J. M. Schnorr, D. van der Zwaag, J. J. Walish, Y. Weizmann, and T. M. Swager, "Sensory arrays of covalently functionalized single-

- walled carbon nanotubes for explosive detection," *Advanced Functional Materials*, vol. 23, no. 42, pp. 5285–5291, 2013.
- [72] K. Jans, K. Bonroy, R. De Palmas, G. Reekmans, H. Jans, W. Laureyn, M. Smet, G. Borghs, and G. Maes, "Stability of mixed PEO - Thiol SAMs for biosensing applications," *Langmuir*, vol. 24, no. 8, pp. 3949– 3954, 2008.
- [73] O. Tomic, H. Ulmer, and J.-e. Haugen, "Standardization methods for handling instrument related signal shift in gas-sensor array measurement data," *Analytica Chimica Acta*, vol. 472, pp. 99–111, 2002.
 [74] K. C. Persaud, "Towards bionic noses," *Sensor Review*, vol. 2, no.
- [74] K. C. Persaud, "Towards bionic noses," Sensor Review, vol. 2, no. 285203, pp. 165–171, 2017.
- [75] G. Sauerbrey, "Use of Quartz Crystal Vibrator for Weighting Thin Films on a Microbalance," *Zeitschrift fur Physik*, vol. 155, pp. 206–222, 1959.
- [76] J. K. K. R. N. J. C. Love, L. A. Estroff and G. M. Whitesides, "Self-assembled monolayers of thiolates on metals as a form of nanotechnology," *Chemical Reviews*, vol. 105, no. 5, 2005.
- [77] J. W. Grate, "Acoustic wave microsensor arrays for vapor sensing," Chemical Reviews, vol. 100, no. 7, pp. 2627–2648, 2000.
- [78] M. L. Johnston, "Thin-film bulk acoustic resonators on integrated circuits for physical sensing applications," 2012.
- [79] B. P. Otis and J. M. Rabaey, "A 300μmW 1.9GHz CMOS oscillator utilizing micromachined resonators," in *European Solid-State Circuits Conference*, vol. 38, no. 7, 2002, pp. 151–154.